Editors' Suggestion

Muon $g-2$ and B Anomalies from Dark Matter

Giorgio Arcadi,[1,2,*] Lorenzo Calibbi,[3,†] Marco Fedele,[4,‡] and Federico Mescia[5,§]
[1]Dipartimento di Matematica e Fisica, Università di Roma 3, Via della Vasca Navale 84, 00146 Roma, Italy
[2]INFN Sezione Roma 3, Via della Vasca Navale 84, 00146 Roma, Italy
[3]School of Physics, Nankai University, Tianjin 300071, China
[4]Institut für Theoretische Teilchenphysik, Karlsruhe Institute of Technology, D-76131 Karlsruhe, Germany
[5]Department de Física Quàntica i Astrofísica, Institut de Ciències del Cosmos (ICCUB), Universitat de Barcelona, Martí i Franquès 1, E-08028 Barcelona, Spain

(Received 23 April 2021; accepted 22 June 2021; published 4 August 2021)

In light of the recent result of the muon $g-2$ experiment and the update on the test of lepton flavor universality R_K published by the LHCb Collaboration, we systematically study for the first time a set of models with minimal field content that can simultaneously give (i) a thermal dark matter candidate; (ii) large loop contributions to $b \to s\ell\ell$ processes able to address R_K and the other B anomalies; (iii) a natural solution to the muon $g-2$ discrepancy through chirally enhanced contributions. Moreover, this type of model with heavy particles and chiral enhancement can evade the strong limits from direct searches but can be tested at present and future colliders and direct-detection searches.

DOI: 10.1103/PhysRevLett.127.061802

Introduction.—The first results of the FNAL muon $g-2$ experiment [1] have confirmed the long-standing discrepancy with the standard model (SM) prediction of the anomalous magnetic moment of the muon $a_\mu \equiv (g-2)_\mu/2$. Taking into account the previous measurement of the BNL experiment [2], the deviation from the theoretical prediction amounts to about 4.2σ:

$$\Delta a_\mu \equiv a_\mu^{\rm exp} - a_\mu^{\rm SM} = 251(59) \times 10^{-11}. \qquad (1)$$

This result drastically reduces the probability of a statistical fluctuation or overlooked systematical effects [3]. It is also unlikely that such a discrepancy can be fully explained by underestimated hadronic uncertainties [4]. Moreover, even if hadronic vacuum polarization effects are assumed to be large enough to account for the anomaly [5], this would cause a deterioration of the electroweak (EW) fit such that tensions of comparable significance in other EW observables would arise [6–9]. Hence this new result strongly supports the case for new physics (NP) requiring, in particular, the presence of new particles with nontrivial interactions with SM muons at scales $\lesssim 100$ TeV [10–12], where the upper bound can be reached only in the presence of fields strongly coupled with muons, and at the price of fine-tuned cancellations between SM and NP contributions to the muon mass.

Interestingly, also the persistent anomalies in semileptonic B meson decays of the kind $b \to s\ell\ell$ seem to point to a NP sector with preferred couplings to muons. In particular, the theoretically clean lepton flavor universality (LFU) ratio $R_K = {\rm BR}(B \to K\mu^+\mu^-)/{\rm BR}(B \to Ke^+e^-)$, for which an updated measurement has been recently released by the LHCb Collaboration, deviates from the SM prediction by more than 3σ [13,14]. Once the analogous LFU test R_{K^*} [21,22] and the branching ratios and angular analysis of other decays mediated by $b \to s\ell\ell$ transitions [23–32] are considered as well, global fits to data prefer the presence of NP contributions at the level of $\gtrsim 5\sigma$ [33–43] compared to the SM prediction only. These anomalies could also be explained by new particles interacting with muons at scales $\lesssim 100$ TeV [44]. A further call for new physics (NP) beyond the standard model (BSM) is represented by the overwhelming evidence for dark matter (DM). The aim of this Letter is to combine an explanation to the muon $g-2$ discrepancy and B anomalies with a viable thermal DM candidate. While the idea of connecting DM with at least one of the anomalies is not new by itself [45–68], this work is, to our knowledge, the first to propose a systematic classification of models that accommodate, with a minimal field content and without fine-tuned choices of the parameters, viable DM phenomenology and the aforementioned anomalies altogether.

Remarkably, the DM "induces" the anomalies since the DM field is present in the Feynman diagrams describing the NP contributions to $(g-2)_\mu$ and $b \to s\mu^+\mu^-$ and the size of the latter depend on the same couplings controlling the DM

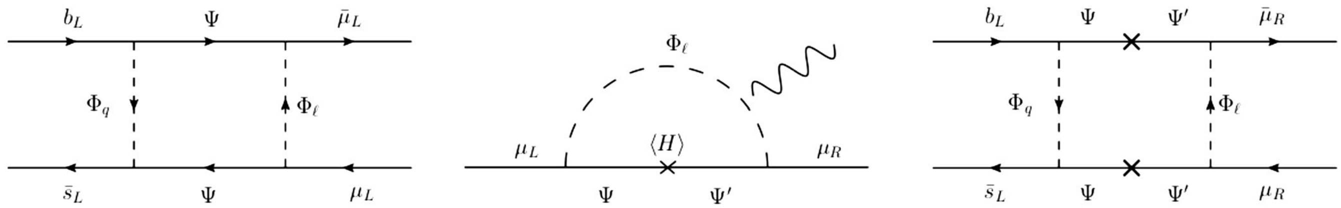

FIG. 1. Basic diagrams providing a contribution to $b\to s\mu\mu$ of the form $\delta C_\mu^9 = -\delta C_\mu^{10}$ (left) or $\delta C_\mu^9 = \delta C_\mu^{10}$ (right). In the middle, an enhanced contribution to $(g-2)_\mu$ is shown. In these examples, the *flavor mediator*, i.e., the field coupling with both quarks and leptons, is a fermion.

relic density. The class of models presented in this work extend the SM spectrum with four NP fields with gauge invariant couplings with the muons, and with second and third generation left-handed quarks. To ensure DM stability, a global (possibly accidental) symmetry, forbidding couplings of the DM with two SM states, should be also enforced [69]. Under these assumptions NP contributions to both a_μ and $b\to s\mu^+\mu^-$ can only occur through loop diagrams, as in the framework discussed in Refs. [70–72], where only NP fields (DM in particular) run in the loop.

Setup.—Recent global analyses of the $b\to s\ell\ell$ data [33–41], including the new measurement of R_K [42,43], show that a satisfactory fit of the observed B anomalies favors solutions featuring NP effects in δC_μ^9 and δC_μ^{10}:

$$\mathcal{H}_{\rm eff} \supset -\frac{4G_F}{\sqrt{2}}\frac{e^2}{16\pi^2}V_{tb}V_{ts}^*[C_\mu^9(\bar{s}\gamma_\mu P_L b)(\bar{\mu}\gamma^\mu\mu) + C_\mu^{10}(\bar{s}\gamma_\mu P_L b)(\bar{\mu}\gamma^\mu\gamma_5\mu) + \text{H.c.}]. \tag{2}$$

The simplest way to address the anomalies is represented by the scenario $\delta C_\mu^9 = -\delta C_\mu^{10}$, corresponding to NP interacting only with left-handed quarks and muons. This solution seems also favored by global fits which points towards a subdominant contribution from hadronic RH currents. As shown in Ref. [66] this scenario can be accommodated by introducing just three BSM fields: two scalars, Φ_q and Φ_ℓ, respectively, coupling to quarks and leptons and a fermion "flavor mediator" Ψ, as in the figure, or alternatively two fermions, Ψ_q and Ψ_ℓ, and a scalar flavor mediator Φ. One of these fields will constitute the DM candidate. B anomalies will be generated by 1-loop diagrams as the one shown in the left panels of Fig. 1. Our analysis in Ref. [66] shows that a satisfactory solution of the B anomalies and of the DM puzzles requires (i) DM to be an $SU(2)_L\times U(1)_Y$ singlet; (ii) the DM field to couple to muons (since the large couplings to muons required by the fit to the B anomalies induce efficient DM annihilation evading the problem of DM overproduction); (iii) DM to be a Majorana fermion, a real scalar, or one of the two components of a complex scalar with a mass splitting $> \mathcal{O}(100)$ keV (such that the most dangerous contributions to DM direct detection are suppressed). The above considerations restrict the set of viable possibilities to cases where the fields Ψ/Φ or Φ_ℓ/Ψ_ℓ are (or mix with) a DM singlet.

The subset of NP fields coupling to muons also contributes to the dipole operator relevant for the muon $g-2$:

$$\mathcal{L} \supset \frac{ev}{8\pi^2}C_{\mu\mu}(\bar{\mu}_L\sigma_{\mu\nu}\mu_R)F^{\mu\nu} + \text{H.c.}$$
$$\Rightarrow \Delta a_\mu = \frac{m_\mu v}{2\pi^2}\text{Re}(C_{\mu\mu}), \tag{3}$$

where v is the SM Higgs vacuum expectation value (vev) $\simeq$246 GeV. Gauge invariance requires a muon chirality flip. Since the NP fields $\Psi-\Phi_\ell$ or $\Phi-\Psi_\ell$ do not couple to RH muons, this can occur only in the external lines, at the price of a suppression, proportional to the muon Yukawa coupling, which marginally provide a viable value for Δa_μ [50]. Hence, a natural solution requires the chirality flip inside the loop [48,50,72,73], i.e., the addition of a 4th field: either Ψ'/Φ' mixing with Ψ/Φ through a Higgs vev, or Φ'_ℓ/Ψ'_ℓ mixing with Φ_ℓ/Ψ_ℓ. This, in turn, implies additional contributions to B anomalies, breaking the relation $\delta C_\mu^9 = -\delta C_\mu^{10}$. Illustrative diagrams are shown in the second and third panel of Fig. 1. The conditions above are satisfied only by some specific combinations, displayed in Table I, of the quantum numbers of the NP fields. In particular, there is a unique choice for the transformation properties under $SU(3)_c$ and only three for $SU(2)_L$. The possible models can be then classified, according to the spin of the NP fields:

$$\text{Class } \mathcal{F}\text{: either}\{\Phi_q,\Phi_\ell,\Phi'_\ell,\Psi\} \quad \text{or} \quad \{\Phi_q,\Phi_\ell,\Psi,\Psi'\}.$$
$$\text{Class } \mathcal{S}\text{: either}\{\Psi_q,\Psi_\ell,\Psi'_\ell,\Phi\} \quad \text{or} \quad \{\Psi_q,\Psi_\ell,\Phi,\Phi'\}.$$

Within each class, we can identify 9 possible options, according to the hypercharge assignments. These are displayed in Table II.

Minimal models.—In the following we characterize in more detail the two classes of models defined above.

Class $\mathcal{F}$: These models feature a vectorlike fermion Ψ as flavor mediator and two extra scalars Φ_q and Φ_ℓ coupling to the SM left-handed fermions. For models with an additional scalar Φ'_ℓ, the Lagrangian is

TABLE I. Possible gauge quantum numbers of the new fields. Our convention for the hypercharge ($Q = Y + T_3$) is such that the SM fields have $Y(Q) = 1/6$, $Y(U) = 2/3$, $Y(D) = -1/3$, $Y(L) = -1/2$, $Y(E) = -1$, $Y(H) = 1/2$. We highlight in green (gray) the combinations that provide a viable simultaneous fit to DM and B-anomalies. Minimal models includes the first three fields plus one chosen from the last two columns.

$SU(3)_c$	Φ_q/Ψ_q	Φ_ℓ/Ψ_ℓ	Ψ/Φ	Φ'_ℓ/Ψ'_ℓ	Ψ'/Φ'
A	**3**	**1**	**1**	**1**	**1**
B	**1**	$\bar{\mathbf{3}}$	**3**	$\bar{\mathbf{3}}$	**3**
$SU(2)_L$	Φ_q/Ψ_q	Φ_ℓ/Ψ_ℓ	Ψ/Φ	Φ'_ℓ/Ψ'_ℓ	Ψ'/Φ'
I	**2**	**2**	**1**	**1**	**2**
II	**1**	**1**	**2**	**2**	**1**
III	**3**	**3**	**2**	**2**	**3**
IV	**2**	**2**	**3**	**3**	**2**
V	**3**	**1**	**2**	**2**	**1**
VI	**1**	**3**	**2**	**2**	**3**
$U(1)_Y$	$1/6 - X$	$-1/2 - X$	X	$-1 - X$	$-1/2 + X$

$$\mathcal{L}_{\mathcal{F}}^{\Phi_\ell\Phi'_\ell} \supset \Gamma_i^Q \bar{Q}_i P_R \Psi \Phi_q + \Gamma_i^L \bar{L}_i P_R \Psi \Phi_\ell + \Gamma_i^E \bar{E}_i P_L \Psi \Phi'_\ell + a_H \Phi_\ell^\dagger \Phi'_\ell H + \text{H.c.}, \quad (4)$$

where a_H is a parameter with a dimension of a mass. In case of Φ'_ℓ being a doublet, one may need to substitute $\Phi'_\ell \to \tilde{\Phi}'_\ell = i\sigma_2 \Phi'_\ell$. Notice that, depending on the hypercharge, either the charged or the neutral components in Φ_ℓ and Φ'_ℓ mix upon EW-symmetry breaking (EWSB). The resulting mass eigenstates will be given by diagonalizing a matrix of the following schematic form: [74]

$$\mathcal{M}_\Phi^2 = \begin{pmatrix} M_{\Phi_\ell}^2 & a_H v/\sqrt{2} \\ a_H^* v/\sqrt{2} & M_{\Phi'_\ell}^2 \end{pmatrix}. \quad (5)$$

TABLE II. Minimal sets of fields fulfilling all requirements listed in the introduction. The fields are denoted by their transformation properties under, respectively, ($\mathrm{SU}(3)_c$, $\mathrm{SU}(2)_L$, $\mathrm{U}(1)_Y$). Models highlighted in cyan (light gray) feature singlet DM, models in red (gray) have singlet-doublet mixed DM.

Label	Φ_q/Ψ_q	Φ_ℓ/Ψ_ℓ	Ψ/Φ	Φ'_ℓ/Ψ'_ℓ	Ψ'/Φ'
$\mathcal{F}_{\rm Ia}/\mathcal{S}_{\rm Ia}$	$(\mathbf{3},\mathbf{2})_{1/6}$	$(\mathbf{1},\mathbf{2})_{-1/2}$	$(\mathbf{1},\mathbf{1})_0$	$(\mathbf{1},\mathbf{1})_{-1}$	–
$\mathcal{F}_{\rm Ib}/\mathcal{S}_{\rm Ib}$	$(\mathbf{3},\mathbf{2})_{1/6}$	$(\mathbf{1},\mathbf{2})_{-1/2}$	$(\mathbf{1},\mathbf{1})_0$	–	$(\mathbf{1},\mathbf{2})_{-1/2}$
$\mathcal{F}_{\rm Ic}/\mathcal{S}_{\rm Ic}$	$(\mathbf{3},\mathbf{2})_{7/6}$	$(\mathbf{1},\mathbf{2})_{1/2}$	$(\mathbf{1},\mathbf{1})_{-1}$	$(\mathbf{1},\mathbf{1})_0$	–
$\mathcal{F}_{\rm IIa}/\mathcal{S}_{\rm IIa}$	$(\mathbf{3},\mathbf{1})_{2/3}$	$(\mathbf{1},\mathbf{1})_0$	$(\mathbf{1},\mathbf{2})_{-1/2}$	$(\mathbf{1},\mathbf{2})_{-1/2}$	–
$\mathcal{F}_{\rm IIb}/\mathcal{S}_{\rm IIb}$	$(\mathbf{3},\mathbf{1})_{2/3}$	$(\mathbf{1},\mathbf{1})_0$	$(\mathbf{1},\mathbf{2})_{-1/2}$	–	$(\mathbf{1},\mathbf{1})_{-1}$
$\mathcal{F}_{\rm IIc}/\mathcal{S}_{\rm IIc}$	$(\mathbf{3},\mathbf{1})_{-1/3}$	$(\mathbf{1},\mathbf{1})_{-1}$	$(\mathbf{1},\mathbf{2})_{1/2}$	–	$(\mathbf{1},\mathbf{1})_0$
$\mathcal{F}_{\rm Va}/\mathcal{S}_{\rm Va}$	$(\mathbf{3},\mathbf{3})_{2/3}$	$(\mathbf{1},\mathbf{1})_0$	$(\mathbf{1},\mathbf{2})_{-1/2}$	$(\mathbf{1},\mathbf{2})_{-1/2}$	–
$\mathcal{F}_{\rm Vb}/\mathcal{S}_{\rm Vb}$	$(\mathbf{3},\mathbf{3})_{2/3}$	$(\mathbf{1},\mathbf{1})_0$	$(\mathbf{1},\mathbf{2})_{-1/2}$	–	$(\mathbf{1},\mathbf{1})_{-1}$
$\mathcal{F}_{\rm Vc}/\mathcal{S}_{\rm Vc}$	$(\mathbf{3},\mathbf{3})_{-1/3}$	$(\mathbf{1},\mathbf{1})_{-1}$	$(\mathbf{1},\mathbf{2})_{1/2}$	–	$(\mathbf{1},\mathbf{1})_0$

For models where instead the fourth field is the additional fermion Ψ' mixing with the flavor mediator Ψ, the Lagrangian schematically reads

$$\mathcal{L}_{\mathcal{F}}^{\Psi\Psi'} \supset \Gamma_i^Q \bar{Q}_i P_R \Psi \Phi_q + \Gamma_i^L \bar{L}_i P_R \Psi \Phi_\ell + \Gamma_i^E \bar{E}_i P_L \Psi' \Phi_\ell + \lambda_L^H \bar{\Psi} P_L \Psi' H + \lambda_{HR} \bar{\Psi} P_R \Psi' H + \text{H.c.}$$

For illustration here we show the case labeled $\mathcal{F}_{\rm IIc}$ in Table II, where Ψ is a doublet and Ψ' a Majorana or Dirac singlet (we recall all the extra fermions, unless they are Majorana, come in vectorlike pairs). We have also omitted couplings to RH quarks, possibly allowed by gauge invariance, of the kind $\Gamma_i^D \bar{D}_i P_R \Psi' \Phi_q$ and $\Gamma_i^U \bar{U}_i P_R \Psi' \Phi_q$ (that we are assuming to be suppressed in the following). For this kind of model the singlet-doublet mass matrix has the following schematic forms:

$$\mathcal{M}_\Psi^M = \begin{pmatrix} M_{\Psi'} & \lambda_L^H v/\sqrt{2} & \lambda_R^H v/\sqrt{2} \\ \lambda_L^H v/\sqrt{2} & 0 & M_\Psi \\ \lambda_R^H v/\sqrt{2} & M_\Psi & 0 \end{pmatrix}, \quad (6)$$

$$\mathcal{M}_\Psi^D = \begin{pmatrix} M_{\Psi'} & \lambda_R^H v/\sqrt{2} \\ \lambda_L^H v/\sqrt{2} & M_\Psi \end{pmatrix}, \quad (7)$$

for, respectively, a Majorana and a Dirac singlet field (Ψ' in this illustrative examples).

Class $\mathcal{S}$: In these models, we introduce a scalar flavor mediator Φ and two fermions Ψ_q and Ψ_ℓ in vectorlike representations of the SM gauge group, plus either an additional Ψ'_ℓ or a Φ'. The Lagrangians and the mass matrices are as those given above *mutatis mutandis*:

$$\mathcal{L}_{\mathcal{S}}^{\Psi_\ell\Psi'_\ell} \supset \Gamma_i^Q \bar{Q}_i P_R \Psi_q \Phi + \Gamma_i^L \bar{L}_i P_R \Psi_\ell \Phi + \Gamma_i^E \bar{E}_i P_L \Psi'_\ell \Phi + \lambda_{H1} \bar{\Psi}_\ell P_R \Psi'_\ell H + \lambda_{H2} \bar{\Psi}_\ell P_L \Psi'_\ell H + \text{H.c.},$$

$$\mathcal{L}_{\mathcal{S}}^{\Phi\Phi'} \supset \Gamma_i^Q \bar{Q}_i P_R \Psi_q \Phi + \Gamma_i^L \bar{L}_i P_R \Psi_\ell \Phi + \Gamma_i^E \bar{E}_i P_L \Psi_\ell \Phi' + a_H \Phi^\dagger \Phi' H + \text{H.c.}$$

Results: $\mathcal{F}_{\rm Ib}$—Singlet-doublet fermionic DM.—To illustrate the phenomenology of our minimal models, we choose as example model $\mathcal{F}_{\rm Ib}$. We add $\mathcal{F}_{\rm IIb}$ in the Supplemental Material [75] (including Ref. [76]). Here, to a Majorana DM, $\Psi = (\mathbf{1}, \mathbf{1}, 0)$, we add a doublet fermion, $\Psi' = (\mathbf{1}, \mathbf{2}, -1/2) = (\Psi'^0, \Psi'^-)$, namely,

$$\mathcal{L}_{\mathcal{F}_{\rm Ib}} \supset \Gamma_i^Q \bar{Q}_i P_R \Psi \Phi_q + \Gamma_i^L \bar{L}_i P_R \Psi \Phi_\ell + \Gamma_i^E \bar{E}_i P_L \Psi' \cdot \Phi_\ell + \lambda_L^H \bar{\Psi} P_L \Psi' \cdot H + \lambda_R^H \bar{\Psi} P_R \Psi' \cdot H + \text{H.c.},$$

where $\Phi_\ell = (\mathbf{1}, \mathbf{2}, -1/2)$, $\Phi_q = (\mathbf{3}, \mathbf{2}, 1/6)$, and the $\mathrm{SU}(2)_L$ contraction $\Psi' \cdot H = \epsilon_{ab} \Psi'_a H_b$ with $\epsilon_{ab} = (i\sigma_2)_{ab}$.

After EWSB, the neutral components of Ψ' and Ψ mix [77] giving three Majorana mass eigenstates, $F^0_{1,2,3}$, with $(\Psi^{0\,c}_R \equiv \Psi^0_L, \Psi'^0_L, \Psi'^{0\,c}_R)^T_i = V_{ij} F^0_{L,j}$ and $(V^T \mathcal{M}^M_\Psi V)_{ij} = \delta_{ij} m^{F^0}_i$.

In terms of the above rotations and mass eigenvalues, the Wilson coefficients for $b \to s\ell\ell$ transitions are

$$\delta C^9_\mu = \mathcal{N} \frac{\Gamma^{Q*}_s \Gamma^Q_b}{32\pi\alpha_{\rm EM}} \sum_{i,j=1}^{3} \frac{V_{1i} V_{1j}}{(m^{F^0}_j)^2} (|\Gamma^L_\mu|^2 V_{1i} V_{1j} - |\Gamma^E_\mu|^2 V_{2i} V_{2j}) D(x_{Qj}, x_{\ell j}, x_{ij}),$$

$$\delta C^{10}_\mu = -\mathcal{N} \frac{\Gamma^{Q*}_s \Gamma^Q_b}{32\pi\alpha_{\rm EM}} \sum_{i,j=1}^{3} \frac{V_{1i} V_{1j}}{(m^{F^0}_j)^2} (|\Gamma^L_\mu|^2 V_{1i} V_{1j} + |\Gamma^E_\mu|^2 V_{2i} V_{2j}) D(x_{Qj}, x_{\ell j}, x_{ij}),$$

where we have defined $x_{Qj} = (m_{\Phi_Q}/m^{F^0}_j)^2$, $x_{\ell j} = (m_{\Phi_\ell}/m^{F^0}_j)^2$, $x_{ij} = (m^{F^0}_i/m^{F^0}_j)^2$, $\mathcal{N}^{-1} = 4G_F/\sqrt{2} V_{tb} V^*_{ts}$ and the loop functions read

$$D(x,y,z) = \frac{x(x+2)\log(x)}{(x-1)(x-y)(x-z)} + \frac{y(y+2)\log(y)}{(y-1)(y-x)(y-z)} + \frac{z(z+2)\log(z)}{(z-1)(z-x)(z-y)}.$$

The dominant effect of our fields on the muon $g-2$ reads

$$\Delta a_\mu \simeq -\frac{m_\mu}{2\pi^2 m^2_{\Phi_\ell}} \sum_{j=1,2,3} m^{F^0}_j {\rm Re}(\Gamma^L_\mu \Gamma^E_\mu V_{1j} V_{2j}) \tilde{H}(x^{-1}_{\ell j}),$$

with $\tilde{H}(x) = (x^2 - 1 - 2x\log x)/[8(x-1)^3]$. See Refs. [50,72] for subdominant terms.

The presence of an $SU(2)_L$ doublet Ψ' causes a notable effect in DM direct detection as it couples to the SM Higgs and Z bosons at the tree level (see Ref. [78]). These same couplings would also lead, for light enough DM, to invisible decays of the Z and Higgs bosons.

The results of our analysis are shown in Fig. 2, in the $(M_\Psi, M_{\Psi'})$ two-dimensional plane, for a sample assignation of the parameters of the model. The region correctly fitting, at 1σ, the muon $g-2$ anomaly is shown as a green band while the one correctly accounting for B anomalies has been marked in orange. Notice that, in our study, we have assumed all the parameters of Ψ, Ψ' mass matrix to be real. The correct DM relic density, if conventional freeze-out is assumed, is achieved only in the narrow red strip. Finally, the blue-hatched region is excluded by constraints from XENON1T [79] on DM SI interactions, while the gray regions correspond to an invisible branching fraction of the Higgs boson above 11% [80], or an invisible width of the Z boson above 2.3 MeV [81]. No analogous constrains from LHC, as the ones considered in Ref. [66], have been shown in the plot since we have chosen benchmark assignations for $m_{\Phi_\ell}, m_{\Phi_q}$ beyond current experimental

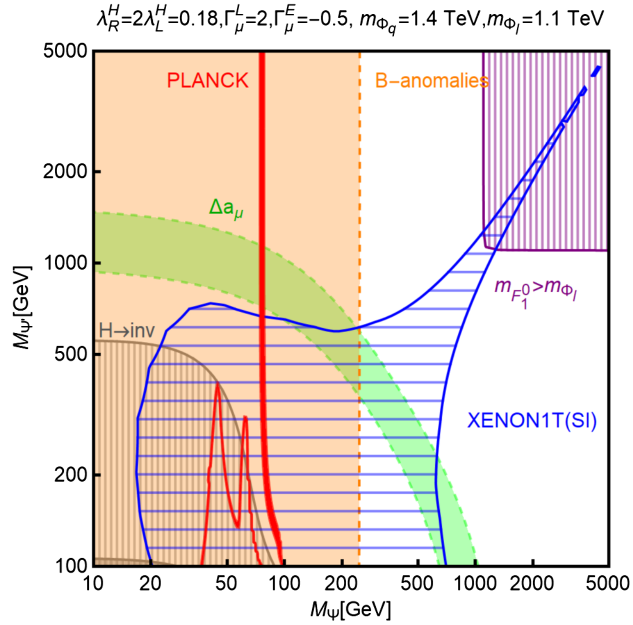

FIG. 2. Summary of results for the model $\mathcal{F}_{\rm Ib}$, in the $(M_\Psi, M_{\Psi'})$ plane for a given parameter set. The quark coupling $\Gamma^{Q*}_s \Gamma^Q_b$ is set to 0.15, according to the $B_s - \overline{B}_s$ constraints as found in Ref. [66]. Green and orange bands account for the $g-2$ (at 1σ) and B anomalies (at 2σ), respectively. The red isocontours correspond to the correct DM relic density from the freeze-out paradigm. The blue hatched regions are excluded by direct detection limits from XENON1T, whereas the gray ones by searches of invisible decays of Higgs and Z bosons.

sensitivity. Additional bounds from the production of the charged and neutral partners of the DM should be considered though, being responsible of 2–3 leptons + missing energy signatures (see, e.g., Ref. [82]). These limits are not competitive with those from invisible decays of the Higgs boson and DM direct detection and, hence, have not been shown. Similarly, constraints from electroweak precision observables have no impact on the parameter space of Fig. 2, as can be seen in the context of a generic fermionic singlet-doublet model, e.g., in Refs. [77,78].

As illustrated by the figure, a combined fit of the $g-2$ and of the B anomalies can be easily achieved, together with the correct DM relic density and without conflicts with experimental exclusions, for $M_\Psi \ll M_{\Psi'}$. This corresponds to a mostly singletlike DM achieving its relic density mostly through annihilations into muon pairs mediated by Φ_ℓ. For this reason the isocontour of the correct relic density appears as a vertical line since the mass of Φ_ℓ and its couplings have been kept fixed in the plot. It is very promising that both anomalies can be accounted for with a standard thermal DM candidate.

Conclusions.—The new results presented by the Muon $g-2$ Collaboration could represent the first departure from the prediction of the standard model observed in a particle physics experiment. This nicely combines with the growing significance of R_K announced by the LHCb Collaboration and the highly significant deviation from the SM prediction obtained by global fits of all $b \to s\ell\ell$ observables. It is very suggestive that both anomalies require nonstandard contributions to operators involving muons. This makes it crucial to find compelling theoretical frameworks where both experimental results can be naturally explained. In this Letter, we have presented a particularly simple setup where this is possible within the context of models that also provide a viable thermal dark matter candidate. We have discussed what are the minimal ingredients and properties that allow us to explain the anomalies through loop effects due to the DM particles and few other BSM fields, being four the minimum number of fields that need to be added to the SM. The general characteristic of this class of models is that the DM phenomenology is controlled by the same parameters that enter the flavor observables. As a consequence, they feature a high degree of correlation among DM, flavor and collider searches and thus an enhanced testability. After a systematic classification of these minimal models based on the quantum numbers of their field content, we have presented an example with $SU(2)_L$ singlet-doublet fermion DM, and a case with real scalar DM in the Supplemental Material [75]. In both examples, a thermal DM candidate can naturally provide a simultaneous explanation of the muon $g-2$ (through chirally enhanced contributions) and the B-physics anomalies, while evading present bounds from collider and DM searches. Despite the simplicity, their rich phenomenology makes it possible to test them, at least in part, at future runs of the LHC and/or DM direct detection experiments. In the long term, as large interactions involving muons are necessary, these minimal DM models would be an ideal target for a multi-TeV muon collider [10–12,83–85].

L. C. is supported by the National Natural Science Foundation of China under the Grant No. 12035008. F. M. acknowledges financial support from the State Agency for Research of the Spanish Ministry of Science and Innovation through the "Unit of Excellence María de Maeztu 2020-2023" award to the Institute of Cosmos Sciences (CEX2019-000918-M) and from PID2019–105614 GB-C21 and 2017-SGR-929 Grants. The work of M. F. is supported by the Deutsche Forschungsgemeinschaft (DFG, German Research Foundation) under Grant 396021762—TRR 257, "Particle Physics Phenomenology after the Higgs Discovery."

Note added in the proof.—A recent discussion about minimal setups attempting a combined explanation to the $(g-2)_\mu$, B-physics and CKM anomalies (not from DM) can be found in Ref. [86].

---

[*]giorgio.arcadi@uniroma3.it
[†]calibbi@nankai.edu.cn
[‡]marco.fedele@kit.edu
[§]mescia@ub.edu

[1] B. Abi *et al.* (Muon g-2 Collaboration), Measurement of the Positive Muon Anomalous Magnetic Moment to 0.46 ppm, Phys. Rev. Lett. **126**, 141801 (2021).
[2] G. W. Bennett *et al.* (Muon g-2 Collaboration), Final report of the Muon E821 anomalous magnetic moment measurement at BNL, Phys. Rev. D **73**, 072003 (2006).
[3] The deviation obtained taking into account only the FNAL data amounts to about 3.3σ.
[4] T. Aoyama *et al.*, The anomalous magnetic moment of the muon in the Standard Model, Phys. Rep. **887**, 1 (2020).
[5] S. Borsanyi *et al.*, Leading hadronic contribution to the muon 2 magnetic moment from lattice QCD, Nature (London) **593**, 51 (2021).
[6] M. Passera, W. J. Marciano, and A. Sirlin, The muon g-2 and the bounds on the Higgs boson mass, Phys. Rev. D **78**, 013009 (2008).
[7] A. Crivellin, M. Hoferichter, C. A. Manzari, and M. Montull, Hadronic Vacuum Polarization: $(g-2)_\mu$ Versus Global Electroweak Fits, Phys. Rev. Lett. **125**, 091801 (2020).
[8] A. Keshavarzi, W. J. Marciano, M. Passera, and A. Sirlin, Muon $g-2$ and $\Delta\alpha$ connection, Phys. Rev. D **102**, 033002 (2020).
[9] B. Malaescu and M. Schott, Impact of correlations between a_μ and α_{QED} on the EW fit, Eur. Phys. J. C **81**, 46 (2021).
[10] R. Capdevilla, D. Curtin, Y. Kahn, and G. Krnjaic, A guaranteed discovery at future Muon colliders, Phys. Rev. D **103**, 075028 (2021).
[11] D. Buttazzo and P. Paradisi, Probing the muon g-2 anomaly at a muon collider, arXiv:2012.02769.
[12] R. Capdevilla, D. Curtin, Y. Kahn, and G. Krnjaic, A No-Lose theorem for discovering the new physics of $(g-2)_\mu$ at muon colliders, arXiv:2101.10334.
[13] R. Aaij *et al.* (LHCb Collaboration), Test of lepton universality in beauty-quark decays, arXiv:2103.11769.
[14] Recent interpretations of this measurement can be found in Refs. [15–20].
[15] A. Angelescu, D. Bečirević, D. A. Faroughy, F. Jaffredo, and O. Sumensari, On the single leptoquark solutions to the B-physics anomalies, arXiv:2103.12504.
[16] G. Hiller, D. Loose, and I. Nišandžić, Flavorful leptoquarks at the LHC and beyond: Spin 1, J. High Energy Phys. 06 (2021) 080.
[17] A. Greljo, P. Stangl, and A. E. Thomsen, A model of muon anomalies, arXiv:2103.13991.
[18] C. Cornella, D. A. Faroughy, J. Fuentes-Martín, G. Isidori, and M. Neubert, Reading the footprints of the B-meson flavor anomalies, arXiv:2103.16558.
[19] J. Kriewald, C. Hati, J. Orloff, and A. M. Teixeira, Leptoquarks facing flavor tests and $b \to s\ell\ell$ after Moriond, arXiv:2104.00015.
[20] A. Carvunis, F. Dettori, S. Gangal, D. Guadagnoli, and C. Normand, On the effective lifetime of $B_s \to \mu\mu\gamma$, arXiv:2102.13390.
[21] R. Aaij *et al.* (LHCb Collaboration), Test of lepton universality with $B^0 \to K^{*0}\ell^+\ell^-$ decays, J. High Energy Phys. 08 (2017) 055.
[22] A. Abdesselam *et al.* (Belle Collaboration), Test of Lepton Flavor Universality in $B \to K^*\ell^+\ell^-$ Decays at Belle, Phys. Rev. Lett. **126**, 161801 (2021).

[23] R. Aaij *et al.*(LHCb Collaboration), Angular analysis of the B^0 to $K^{*0}e^+e^-$ decay in the low-q^2 region, J. High Energy Phys. 04 (2015) 064.

[24] R. Aaij *et al.* (LHCb Collaboration), Angular analysis and differential branching fraction of the decay $B_s^0 \to \phi\mu^+\mu^-$, J. High Energy Phys. 09 (2015) 179.

[25] V. Khachatryan *et al.* (CMS Collaboration), Angular analysis of the decay $B^0 \to K^{*0}\mu^+\mu^-$ from pp collisions at $\sqrt{s} = 8$ TeV, Phys. Lett. B **753**, 424 (2016).

[26] R. Aaij *et al.*(LHCb Collaboration), Angular analysis of the $B^0 \to K^{*0}\mu^+\mu^-$ decay using 3 fb^{-1} of integrated luminosity, J. High Energy Phys. 02 (2016) 104.

[27] R. Aaij *et al.* (LHCb Collaboration), Measurements of the S-wave fraction in $B^0 \to K^+\pi^-\mu^+\mu^-$ decays and the $B^0 \to K^*(892)^0\mu^+\mu^-$ differential branching fraction, J. High Energy Phys. 11 (2016) 047; Erratum, J. High Energy Phys. 04 (2017) 142.

[28] S. Wehle *et al.* (Belle Collaboration), Lepton-Flavor-Dependent Angular Analysis of $B \to K^*\ell^+\ell^-$, Phys. Rev. Lett. **118**, 111801 (2017).

[29] A. M. Sirunyan *et al.* (CMS Collaboration), Measurement of angular parameters from the decay $B^0 \to H^{*0}\mu^+\mu^-$ in proton-proton collisions at $\sqrt{s} = 8$ TeV, Phys. Lett. B **781**, 517 (2018).

[30] M. Aaboud *et al.* (ATLAS Collaboration), Angular analysis of $B_d^0 \to K^*\mu^+\mu^-$ decays in pp collisions at $\sqrt{s} = 8$ TeV with the ATLAS detector, J. High Energy Phys. 10 (2018) 047.

[31] R. Aaij *et al.*(LHCb Collaboration), Measurement of *CP*-Averaged Observables in the $B^0 \to K^{*0}\mu^+\mu^-$ Decay, Phys. Rev. Lett. **125**, 011802 (2020).

[32] R. Aaij *et al.* (LHCb Collaboration), Angular Analysis of the $B^+ \to K^{*+}\mu^+\mu^-$ Decay, Phys. Rev. Lett. **126**, 161802 (2021).

[33] G. D'Amico, M. Nardecchia, P. Panci, F. Sannino, A. Strumia, R. Torre, and A. Urbano, Flavour anomalies after the R_{K^*} measurement, J. High Energy Phys. 09 (2017) 010.

[34] M. Ciuchini, A. M. Coutinho, M. Fedele, E. Franco, A. Paul, L. Silvestrini, and M. Valli, New physics in $b \to s\ell^+\ell^-$ confronts new data on Lepton Universality, Eur. Phys. J. C **79**, 719 (2019).

[35] M. Algueró, B. Capdevila, A. Crivellin, S. Descotes-Genon, P. Masjuan, J. Matias, M. Novoa Brunet, and J. Virto, Emerging patterns of New Physics with and without Lepton Flavour Universal contributions, Eur. Phys. J. C **79**, 714 (2019); Eur. Phys. J. C **80**, 511(A) (2020).

[36] A. K. Alok, A. Dighe, S. Gangal, and D. Kumar, Continuing search for new physics in $b \to s\mu\mu$ decays: Two operators at a time, J. High Energy Phys. 06 (2019) 089.

[37] A. Datta, J. Kumar, and D. London, The B anomalies and new physics in $b \to se^+e^-$, Phys. Lett. B **797**, 134858 (2019).

[38] J. Aebischer, W. Altmannshofer, D. Guadagnoli, M. Reboud, P. Stangl, and D. M. Straub, *B*-decay discrepancies after Moriond 2019, Eur. Phys. J. C **80**, 252 (2020).

[39] K. Kowalska, D. Kumar, and E. M. Sessolo, Implications for new physics in $b \to s\mu\mu$ transitions after recent measurements by Belle and LHCb, Eur. Phys. J. C **79**, 840 (2019).

[40] M. Ciuchini, M. Fedele, E. Franco, A. Paul, L. Silvestrini, and M. Valli, Lessons from the $B^{0,+} \to K^{*0,+}\mu^+\mu^-$ angular analyses, Phys. Rev. D **103**, 015030 (2021).

[41] T. Hurth, F. Mahmoudi, and S. Neshatpour, Model independent analysis of the angular observables in $B^0 \to K^{*0}\mu^+\mu^-$ and $B^+ \to K^{*+}\mu^+\mu^-$, Phys. Rev. D **103**, 095020 (2021).

[42] W. Altmannshofer and P. Stangl, New physics in rare B decays after Moriond 2021, arXiv:2103.13370.

[43] L.-S. Geng, B. Grinstein, S. Jäger, S.-Y. Li, J. Martin Camalich, and R.-X. Shi, Implications of new evidence for lepton-universality violation in $b \to s\ell^+\ell^-$ decays, arXiv: 2103.12738.

[44] L. Di Luzio and M. Nardecchia, What is the scale of new physics behind the *B*-flavour anomalies?, Eur. Phys. J. C **77**, 536 (2017).

[45] G. Bélanger, C. Delaunay, and S. Westhoff, A dark matter relic from muon anomalies, Phys. Rev. D **92**, 055021 (2015).

[46] G. Arcadi, M. Dutra, P. Ghosh, M. Lindner, Y. Mambrini, M. Pierre, S. Profumo, and F. S. Queiroz, The waning of the WIMP? A review of models, searches, and constraints, Eur. Phys. J. C **78**, 203 (2018).

[47] J. Kawamura, S. Okawa, and Y. Omura, Interplay between the b $\to s\ell\ell$ anomalies and dark matter physics, Phys. Rev. D **96**, 075041 (2017).

[48] K. Kowalska and E. M. Sessolo, Expectations for the muon g-2 in simplified models with dark matter, J. High Energy Phys. 09 (2017) 112.

[49] J. M. Cline and J. M. Cornell, $R(K^{(*)})$ from dark matter exchange, Phys. Lett. B **782**, 232 (2018).

[50] L. Calibbi, R. Ziegler, and J. Zupan, Minimal models for dark matter and the Muon g − 2 anomaly, J. High Energy Phys. 07 (2018) 046.

[51] B. Barman, D. Borah, L. Mukherjee, and S. Nandi, Correlating the anomalous results in $b \to s$ decays with inert Higgs doublet dark matter and muon $(g-2)$, Phys. Rev. D **100**, 115010 (2019).

[52] B. Grinstein, S. Pokorski, and G. G. Ross, Lepton non-universality in *B* decays and fermion mass structure, J. High Energy Phys. 12 (2018) 079.

[53] D. G. Cerdeño, A. Cheek, P. Martín-Ramiro, and J. M. Moreno, *B* anomalies and dark matter: A complex connection, Eur. Phys. J. C **79**, 517 (2019).

[54] N. Okada and O. Seto, Inelastic extra $U(1)$ charged scalar dark matter, Phys. Rev. D **101**, 023522 (2020).

[55] K. A. Mohan, D. Sengupta, T. M. P. Tait, B. Yan, and C. P. Yuan, Direct detection and LHC constraints on a *t*-channel simplified model of Majorana dark matter at one loop, J. High Energy Phys. 05 (2019) 115.

[56] D. Guadagnoli, M. Reboud, and P. Stangl, The dark side of 4321, J. High Energy Phys. 10 (2020) 084.

[57] A. Carvunis, D. Guadagnoli, M. Reboud, and P. Stangl, Composite dark matter and a horizontal symmetry, J. High Energy Phys. 02 (2021) 056.

[58] A. Biswas and A. Shaw, Reconciling dark matter, $R_{K^{(*)}}$ anomalies and $(g-2)_\mu$ in an $L_\mu - L_\tau$ scenario, J. High Energy Phys. 05 (2019) 165.

[59] L. Calibbi, T. Li, Y. Li, and B. Zhu, Simple model for large *CP* violation in charm decays, *B*-physics anomalies,

muon $g-2$ and dark matter, J. High Energy Phys. 10 (2020) 070.
[60] L. Darmé, M. Fedele, K. Kowalska, and E. M. Sessolo, Flavour anomalies from a split dark sector, J. High Energy Phys. 08 (2020) 148.
[61] J. Kawamura, S. Okawa, and Y. Omura, Current status and muon $g-2$ explanation of lepton portal dark matter, J. High Energy Phys. 08 (2020) 042.
[62] D. Huang, A. P. Morais, and R. Santos, Anomalies in B-meson decays and the muon $g-2$ from dark loops, Phys. Rev. D **102**, 075009 (2020).
[63] S. Okawa and Y. Omura, Light mass window of lepton portal dark matter, J. High Energy Phys. 02 (2021) 231.
[64] K. Kowalska and E. M. Sessolo, Minimal models for $g-2$ and dark matter confront asymptotic safety, arXiv:2012.15200 [Phys. Rev. D (to be published)].
[65] F. D'Eramo, N. Košnik, F. Pobbe, A. Smolkovič, and O. Sumensari, Leptoquarks and real singlets: A richer scalar sector behind the origin of dark matter, arXiv:2012.05743.
[66] G. Arcadi, L. Calibbi, M. Fedele, and F. Mescia, Systematic approach to B-physics anomalies and t-channel dark matter, arXiv:2103.09835.
[67] M. Becker, D. Döring, S. Karmakar, and H. Päs, Fermionic singlet dark matter in one-loop solutions to the R_K anomaly: A systematic study, arXiv:2103.12043.
[68] W. Yin, Radiative lepton mass, and muon $g-2$ with suppressed lepton flavor and CP violations, arXiv:2103.14234.
[69] As by-product, this symmetry forbids mixing among SM and NP fields and, in combination with the gauge symmetries, prevents interactions that would break the baryon and lepton number.
[70] B. Gripaios, M. Nardecchia, and S. Renner, Linear flavour violation and anomalies in B physics, J. High Energy Phys. 06 (2016) 083.
[71] P. Arnan, L. Hofer, F. Mescia, and A. Crivellin, Loop effects of heavy new scalars and fermions in $b \to s\mu^+\mu^-$, J. High Energy Phys. 04 (2017) 043.
[72] P. Arnan, A. Crivellin, M. Fedele, and F. Mescia, Generic loop effects of new scalars and fermions in $b \to s\ell^+\ell^-$ and a vector-like 4$^{\rm th}$ generation, J. High Energy Phys. 06 (2019) 118.
[73] A. Crivellin, M. Hoferichter, and P. Schmidt-Wellenburg, Combined explanations of $(g-2)_{\mu,e}$ and implications for a large muon EDM, Phys. Rev. D **98**, 113002 (2018).
[74] Note that the coupling a_H is bounded by requiring the scalar fields not to develop $\mathrm{SU}(2)_L$-breaking (or even charge-breaking) minima. In the typical parameter space of our models this bound would be of the order 100 GeV, more than sufficient to provide the contribution to the muon $g-2$ with the required chiral enhancement. Indeed, in a similar setup [59], $a_H \sim 20$ GeV has been shown to give a good fit of the muon $g-2$ (for masses of the scalars up to 1 TeV).
[75] See Supplemental Material at http://link.aps.org/supplemental/10.1103/PhysRevLett.127.061802 for the phenomenological analysis of model $\mathcal{F}_{\rm IIb}$.
[76] A. Berlin, D. Hooper, and S. D. McDermott, Simplified dark matter models for the galactic center gamma-ray excess, Phys. Rev. D **89**, 115022 (2014).
[77] L. Calibbi, A. Mariotti, and P. Tziveloglou, Singlet-doublet model: Dark matter searches and LHC constraints, J. High Energy Phys. 10 (2015) 116.
[78] G. Arcadi, A. Djouadi, and M. Raidal, Dark Matter through the Higgs portal, Phys. Rep. **842**, 1 (2020),
[79] E. Aprile *et al.*(XENON Collaboration), Dark Matter Search Results from a One Ton-Year Exposure of XENON1T, Phys. Rev. Lett. **121**, 111302 (2018).
[80] G. Arcadi, A. Djouadi, and M. Kado, The Higgs-portal for dark matter: Effective field theories versus concrete realizations, arXiv:2101.02507.
[81] M. Carena, A. de Gouvea, A. Freitas, and M. Schmitt, Invisible Z boson decays at e+ e- colliders, Phys. Rev. D **68**, 113007 (2003).
[82] G. Aad *et al.* (ATLAS Collaboration), Search for chargino-neutralino production with mass splittings near the electroweak scale in three-lepton final states in $\sqrt{s} = 13$ TeV pp collisions with the ATLAS detector, Phys. Rev. D **101**, 072001 (2020).
[83] W. Yin and M. Yamaguchi, Muon $g-2$ at multi-TeV muon collider, arXiv:2012.03928.
[84] N. Chen, B. Wang, and C.-Y. Yao, The collider tests of a leptophilic scalar for the anomalous magnetic moments, http://arxiv.org/abs/2102.05619.
[85] H. A. Ali *et al.*, The Muon Smasher's guide, arXiv:2103.14043.
[86] D. Marzocca and S. Trinopoulos, following Letter, Minimal Explanation of Flavor Anomalies: B-Meson Decays, Muon Magnetic Moment, and the Cabibbo Angle, Phys. Rev. Lett. **127**, 061802 (2021).